We are IntechOpen, the world's leading publisher of Open Access books Built by scientists, for scientists

4,800
Open access books available

122,000
International authors and editors

135M
Downloads

Our authors are among the

154
Countries delivered to

TOP 1%
most cited scientists

12.2%
Contributors from top 500 universities

CLARIVATE ANALYTICS BOOK CITATION INDEX INDEXED

WEB OF SCIENCE™

Selection of our books indexed in the Book Citation Index in Web of Science™ Core Collection (BKCI)

Interested in publishing with us?
Contact book.department@intechopen.com

Numbers displayed above are based on latest data collected.
For more information visit www.intechopen.com

Chapter 10

Impact of Agricultural Traffic and Tillage Technologies on the Properties of Soil

Ioan Tenu, Petru Carlescu, Petru Cojocariu and Radu Rosca

Additional information is available at the end of the chapter

http://dx.doi.org/10.5772/47746

1. Introduction

Soil has an essential part in preserving life on earth. The main function of soil lies in the fact that it represents the support for the agriculture practice, aiming to insure the peoples' alimentary security and safety, due to its physical and biological properties, to its fertility, to its capacity to provide plants with the water and nutrients needed for their growth.

Taking into account the intensive development of agriculture, the concept of "sustainable development" is a new and complex one, imposed to humanity by the need for the preservation of the soil functions and which is connected not only to agriculture but also to other knowledge fields.

Within the frame of this concept, a special place belongs to sustainable agriculture, which constitutes a system of technologies and good practices aiming not only towards better productions but also to achieve conservative goals.

The main objectives of sustainable agriculture are:

- alimentary safety, by providing the human needs with the necessary food and fiber;
- preservation of the quality of the environment and of the natural resources vital to the agriculture;
- more efficient use of the renewable and non-renewable resources.

In essence, sustainable agriculture must harmoniously combine the three main dimensions: economical, social and ecological.

In order to achieve the goals of sustainable agriculture, the way in which soil tillage works are fulfilled is of an extreme importance, because the induced physical and mechanical changes affect the soil's physical, chemical and biological processes. This is the reason why the concept of "conservative agriculture" (CA) was developed, as a part of the sustainable

agriculture systems, which is based on the use of natural renewable resources, especially soil, and on real time soil regeneration; some complementary agricultural practices are included herein [9, 17]:

- minimum soil disturbance (through reduced soil tillage works and stubble seeding), in order to preserve the soil's structure, fauna and organic matter;
- permanent soil coating (covering crops, residue, mulch), in order to protect it and contribute to the weeds removal;
- different crops rotation and combination schemes, in order to stimulate soil microorganisms and to remove weeds, diseases and pests.

Hence, conservative agriculture is based on an unconventional soil tillage system, named "Soil conservation tillage system" (SCTS). Within this system, moldboard plowing is deferred (completely or partially), the number of agricultural operations is limited and at least 15...30% of the vegetable debris is kept on the soil surface. Worldwide, this system is used on nearly 45% of the farmland, and an increase to 60% is appraised for the next twenty years [9, 17]. The unconventional soil tillage system consists of very different methods, starting with the seeding in the untilled soil and ending with the deep loosening without furrow overturning. Between these two extreme methods, many other variants are possible: reduced tillage, minimum tillage (when up to 30% of the vegetable debris is left on the soil surface), minimum tillage with vegetable mulch (more than 30% of the vegetable debris is left on the soil surface), ridge seeding, partial or strip tillage etc. [9]

As a result, three directions were outlined in order to define the unconventional soil tillage systems:

- direct sowing, when seeds are inserted into the practically non-tilled soil. In this case, soil is tilled only in order to create very small gutter, using small knives mounted on the seeding machine.
- minimum tillage or reduced tillage. In this case, the fact that different types of soil must be differently loosened, in order to favor the normal plant growth, is taken into account. The minimum tillage system includes either the base soil loosening, without furrow overturn, or the superficial tillage, followed by seeding. Sometimes, a minimum of mechanical works is required in order to destroy the weeds, to favor some biologic processes and to support the development of the roots. This system allows the reduction of the energy consumption and working time.
- "rotation" tillage represents another possibility to diminish the intensity of soil loosening. In this case, tillage should be very well correlated with crop rotation. This system is characterized by some peculiarities: the different plants, which are grown in a crop rotation system, have different requirements regarding the soil tillage system; soil requirements towards the tillage system are different from one crop to another; soil characteristics are gradually changing (in a favorable or unfavorable way). It is important to notice that the soil tillage system should be modified according to requirements of the respective crop.

2. Aggressiveness of wheels and active parts of the agricultural units towards soil

Soil degradation is one of the most important problems to be faced nowadays. It is appraised that 5-7 mha of soil are degrading worldwide each year, with a tendency to attend 10 mil. ha per year in the near future [8]. Soil degradation may be physical, chemical and biological. In the case of the physical soil degradation, two important features are affected: bulk density and structure. This means that bulk density increases (the soil is compacted) and the structural elements are damaged (deformed, crushed, sheared, broken, fragmented) [4, 12, 15].

2.1. Effect of agricultural traffic over soil

Mechanization of the agricultural processes and the use of heavy productive units, with high working width, resulted, over time, in soil compaction and reduction of harvest. The use of the organic fertilizers and deep tillage finally results in the diminishing of the content of organic matter and in an increased sensibility to compaction [20].

Soil compaction processes. Soil compaction may be defined as "the compaction of soil mass in a smaller volume". The increase of the bulk density is accompanied by structural changes, changes in the thermal and hydraulic conductivity and in the gas transfer characteristics, all of them affecting the chemical and biological equilibrium of soil.

The artificial (anthropic) soil compaction is the result of exaggerated traffic imposed by agricultural operations, transport operations etc. The intensity of anthropic compaction depends on different factors. Some of them belong to soil, namely to its susceptibility to compaction: uneven grain size distribution, unstable structure, reduced humus content etc. Other factors are influenced by the characteristics of the agricultural equipment; this compaction is favored by the heavy machineries exerting high pressure over soil, by the increased number of passings, by the increased tire air pressure, by the agricultural traffic performed over wet soil etc.

The effects of soil compaction. Soil compaction leads to the reduction of harvest by 50%, compared to the non-compacted soil, while fuel consumption is expected to be increased by 35% [2]. Soil compaction is one of the main causes of surface flow and erosion. In the meantime, compacted soils require higher costs of the irrigation arrangements and exploitation, due to the poor infiltration of water and to the intensified evapotranspiration. Soil compaction also causes the reduction of the water holding capacity and of the permeability, reduces soil aeration, significantly increases the penetration resistance and plowing resistance, inhibits the development of the plant roots and the quality of the ploughland deteriorates. It was established that not only the active parts of the tillage equipment deteriorate the soil structure, but also the tractors' wheels and the tracking wheels of the agricultural machinery; the use of heavier equipments leads to contact pressures of 0.2...1.8 MPa, while the specific resistance of the soil's structure elements is lower than 0.1 MPa (usually 0.02...0.006 MPa); as a result, soil compaction occurs up to 30-50 cm under the tracking wheel and on an area with a width four times the wheel width [6].

Plant and response to compaction. In compacted soils or compacted layers the penetration depth of the roots and their density are restricted, the effect being a slow development of the root system. As a result, the plant's access to water and nutrients is limited, while the capacity of the root system to counteract the noxious effect of pathogenic agents is diminished. This is why plant species with deep roots are less sensible to compaction. Compaction induces changes in the soil's water and air regime, also affecting the activity of microorganisms. Soil compaction also favors the ammonia nitrogen in the detriment of nitric nitrogen, with unfavorable effects over the harvest [10].

Effect of soil tillage over compaction. The agricultural operations related to soil are: ploughing, land preparation, seeding and some of the maintenance operations. In most of the cases, the aim of these operations is to loosen the compacted soil layers. Where soil compaction is a problem, tillage has an ameliorative effect. Soils are usually subjected to two types of traffic: one that produces compaction (wheel traffic) and another one that produces loosening (tillage traffic). Soil reaction to compaction depends on traffic characteristics, soil properties and humidity when the traffic takes place; soil compaction is usually expressed by the means of bulk density, porosity or penetration resistance. Because of wheeled traffic the bulk density of soil increases; the magnitude of the density change depends on the soil texture, its humidity, the wheel-soil contact pressure and the number of passages. The maximum compaction effect is reached when wheel slip reaches 15...25%, due to the fragmentation of the structure elements under the effect of shear stress [18].

2.2. Aggressiveness of the tillage active parts towards soil

Unlike the wheels (tracking wheels, driving wheels etc.), which compact the soil, the active parts of the tillage equipment (rotary cultivator tines, plow shares, cultivator tines etc.) loosen the soil; the rollers, the combined seedbed preparation devices and the combined cultivator are exceptions [6].

In the case of the active parts used for seedbed preparation, their destructive action over the soil structure elements is of an utmost importance. The active parts destroy, to a greater or a lesser extent, the structure elements through deformation, crumbling, cutting, breaking-up. The destruction of the soil's structure is a general phenomenon, occurring at any tillage operation, but it gets large proportions in soils with a rough texture or average-rough texture (sandy soils, sand-loamy soils, clay-loamy soils) for which the mechanical stability of the structure elements is lower, due to the lower clay content. The recently tilled soils, the humid soils or the dry clay soils on which loosening is obtained by the means of rotating active parts (disc harrows, rotary cultivators) are also vulnerable [4].

It should be emphasized that not only the active parts of the tillage equipments destroy the soil's structure, but also the wheels of the tractors or the tracking wheels of the agricultural machinery. In this case, the wheel-soil contact pressure produces compaction as a result of the deformation and breaking-up of the structure elements. The division of the structure elements into fragments results in the increase of the bulk density because of a more stuffed

settlement. Consequently, the soil's capacity to drain and store water is diminished, the thermal regime worsens, the accessibility of plants to nutrients is diminished and the activity of the anaerobic microorganisms is reduced; on sloping lands, the erosion due to water is intensified, and the plants have difficulties in developing the root system, loose their stability and harvest is diminished [14].

Effect of the moldboard plough over soil. In the working process, the plough's share cuts the furrow horizontally and begins its detachment, overturning and lateral displacement, the process being finalized by the moldboard. These actions cause complex deformations of the soil slice, resulting in it's the fragmentation and crumbling. It should be emphasized that, under the action of the share's cutting edge, a number of soil's structural elements are also cut. In the meantime, the twisting of the furrow, both vertically and horizontally, as well as the friction between soil and the parts of the plough body results in the destruction of a number of the structural elements through deformation, crumbling, breaking, fragmentation. The process of destruction of the structure elements is strengthened by the working speed and by the use of worn shares or aggressive moldboards (cylindrical or helical moldboards).

Effect of the rotary cultivators over soil. In the working process, due to the advance movement of the equipment and the rotation movement of the rotor, the active parts penetrate into the soil and cut slices with a particular shape. Under the action of centrifugal force, the soil slices are thrown over the inner surface of the housing and louver. As a result, a supplementary crumbling is achieved, the soil being left behind the rotary harrow in a loosened and fine layer.

The cutting edges of the tines of the rotary harrow cut some of the soil's structural elements, which are also destroyed through deformation, breaking, fragmentation, crumbling, due to the peripheral speed of the tines, to the friction between tines and soil and to the impact between the slices and the housing of the rotary harrow. Pulverization of the structural elements may also occur, when some of them are fragmented to the maximum extent, resulting in particles of clay, silt and sand [19].

When using rotary harrows for the seedbed preparation care should be taken so that the width of the soil slices should not be less than 25 mm. In the working process, the number of destroyed structural elements increases when the slices get thinner. Therefore, the peripheral speed of the tines should no exceed 6 m/s, while the speed of the advance movement should not exceed 1 m/s.

Effect of the disc harrows over soil. The active parts of these agricultural equipments are spherical discs. In the tillage process, the disc is displaced forward, following the movement of the equipment; in the same time, the disc is rotating, due to the contact with the soil. Over the effect of weight, the disc penetrates into the soil and cuts a soil layer, which is raised over the interior concave surface of the disc, is crumbled, displaced laterally and partially overturned. The aggressiveness of the discs depends on their shape, as well as on the cutting angle (disk angle), which can be adjusted between 15 and 30 degrees; crumbling increases when the cutting angle increases.

During the working process, the cutting edge of the disc cuts some of the soil's structural elements; the number of cut structural elements is higher when the disk's cutting edge is indented. In the meantime, the bending of the soil layer, vertically and horizontally, its twisting, as well as the friction between soil and disk, cause the destruction of some structural elements, through deformation, breaking, fragmentation. The proportion of damaged structural elements increases with speed [22].

Effect of the cultivators over soil. Depending on their destination, cultivators are equipped with different types of active parts, the more important being the ones used for weed cutting and for soil loosening.

The weed cutting active parts are aimed to cut the weeds and loosen the soil. During the working process of the arrow type tines, soil is cut horizontally, at a certain depth; in the meantime, the weeds are cut and soil is loosened and crumbled.

The straight, chisel, diamond pointed and narrow arrow type loosening active parts are mounted on rigid or elastic holders. When elastic holders are used, the active part vibrates, exerting an energetic action over soil. As a result of the displacement of these active parts, the superficial soil layer is crumbled and loosened.

The weed cutting type active parts cut some of the soil's structural elements. All the types of active parts (for both weed cutting and soil loosening) destroy the structural elements due to the advance movement, friction, breaking of soil layers, vibration; the structural elements are destroyed through deformation, crumbling, breaking, fragmentation. In order to diminish these adverse effects, speed should be limited to 10-12 km/h.

3. Simulation of the tire wheel-soil and active parts-soil interaction, in laboratory conditions

3.1. Design and testing of a laboratory soil channel test rig

Physical degradation of the soil, caused by the interaction with the active parts and support wheels of the agricultural equipment, refers especially to structural deterioration and its compaction. In order to quantify these issues studies must be performed in order to establish the critical values of the working parameters (of the active parts and wheels) leading to the physical degradation of the soil. In the meantime, correlations should be established between the above-mentioned parameters and the ones characterizing soil structure and compaction.

With the purpose to perform these studies a laboratory test rig for the study of the interaction between the active parts and wheels of agricultural equipment, on one hand, and soil, on the other hand, was designed and built. The designing process has taken into account the similarity laws, in order to reproduce in laboratory conditions the complex processes occurring at the contact interface between the working parts and soil and between the wheels of the agricultural equipments and soil.

The test rig (Figure 1) consists of a rigid frame (1), the soil bin (2), the carriage (3), on which the active part (plough body) for soil working is mounted (6), the wheel with tire (7) and the drum for leveling - settling (8); at the end of laboratory test rig a winch is fixed, which is for trolley carriage with the cable (5). Due to its length (10240 mm), the soil bin is composed of five sections, joined together with screws. The bin was coated, at the inside, with a plastic sheet.

An electric motor (9) and a cylindrical gear (10) are used to drive the drum (11); the drum drives the cable (5), thus towing the cart (3). The ends of the traction cable are attached to the carriage by the means of the load cells (4).

The carriage is also fitted with an electric motor (12) and a gear transmission in order to drive the tire wheel (7). The working depth of the active body can be adjusted by the means of the screw mechanism (13). The screw mechanism (14) is used to adjust the vertical position of the tire wheel; the screw mechanism (15) is used to change the vertical position of the soil leveling and compaction drum. The soil leveling and compaction roller (8), mounted on the carriage, is used to achieve a certain soil compaction, before it is processed by the active body or performing various experiments with the tire wheel.

Four upper trundles – two in the front and two in the back – and four lower trundles - also two in the front and two in the back - are mounted on the carriage frame; the trundles are rolling on rails, mounted on each side of the soil channel frame.

When the carriage is towed by the means of the cable, the wheel (7) rotates due to the interaction with the soil and thus the conditions for a driven tractor wheel are simulated. When the carriage is not towed, the wheel (7) becomes a driving one, being driven by the electrical motor (12) by the means of a cylindrical gear drive and of a trapezoidal belt drive. Thus, the driving wheel of the tractor is simulated.

The towing cable is connected to the carriage by the means of two 1000 daN strain gauge load cells, allowing the measurement of the traction force needed to displace the carriage; the transducers are fitted with spherical joints at both ends and are connected to a programmable weighing controller, which displays the mean values of the corresponding sampling signal and eliminates the load spikes that could occur due to vibrations and soil unevenness.

A control panel (18) is used for the power supply of the two electric motors; the electric cables are guided by the steel cable (16), fixed between the pillars (17). The electrical motors are controlled by the means of a frequency converter, allowing the adjustment of the rotation speed when the frequency is modified between 3 and 50 Hz. The dynamic braking principle is used in order to stop the carriage at the end of travel. Switches on the control panel allow the selection of the electric motor (the carriage towing motor or the tire wheel driving motor), as well as its forward or reverse motion.

A bill chernozem type of soil was used to fill the soil channel bin, having a loam-clay texture, the aggregate size of 0.02 ... 50 mm and 17-19% humidity.

3.2. Laboratory tests concerning some active parts and tire wheels

The test rig was tested in two phases. In the first phase, the laboratory test rig (soil channel) was tested to see if the prescribed constructive-functional parameters are attained. It was found that the test rig has the following constructive-functional parameters: depth of active enforcement machinery of working the soil: 0 ... 300 mm; adjustment of working angle of the active part relative to the soil surface: (-) 25^0 ... (+) 25^0; the speed of the carriage when it is hauled by the 5,5 kW electric motor: 0,5 ... 1,55 m/s (1,8 ... 5,58 km/h); the maximum pull-down force for the with tire wheel and the soil leveling and settlement drum: 500 daN; maximum traction force of the cable (of the carriage), at a speed of the trolley of 0,55 m/s: 800 daN; maximum traction force of the cable (of the carriage) at a speed of the carriage of 1,55 m/s: 280 daN; cable breakdown point: 40,83 kN. It was concluded that there were no significant differences between the design parameters and the achieved ones.

In the second phase, the laboratory test rig was used in order to study the soil - moldboard plough body interaction and the tire wheel-soil interaction (Figure 2).

The studies concerning the active part-soil interaction were performed over a semi helical moldboard plough body, with a working width of 200 mm. The plough body was mounted on the carriage of the test rig. The influence of working depth, soil resistance to penetration and travel speed on the traction resistance and specific power consumption were evaluated. The results presented in the Table 1 show that increasing the traveling speed of the plough body results in an increased traction resistance. In the meantime, as the plough body speed increases, the specific power consumption significantly increases.

When soil penetration resistance increases, the traction force and specific power consumption also increase.

As far as the working depth is concerned, it was concluded that the increase of the penetration depth of the plough body resulted in a significant increase of traction resistance.

It was also noticed that increasing the working depth of the plough body resulted in an uneven change of the specific power consumption: increasing the working depth from 100 mm to 150 mm caused a slight decrease of the specific power consumption; when the working depth was further increased from 150 mm to 200 mm, the specific power consumption increased. These variations of the power specific consumption could be explained as follows: for small working depths (below 15 cm) the soil slice was not yet deployed as furrow and was not overturned, so that the specific power consumption was low; for depths over 15 cm the conditions to overturn the furrow were better, so that supplementary power was consumed in order to overturn it.

In the series of experiments regarding the driving wheel mounted on the test rig, the tire wheel was used to drive the carriage along the soil channel, the wheel being driven by the 3 kW electric motor. The wheel was equipped with a 5.00-12/4PR TA60 traction tire (with angled lugs).

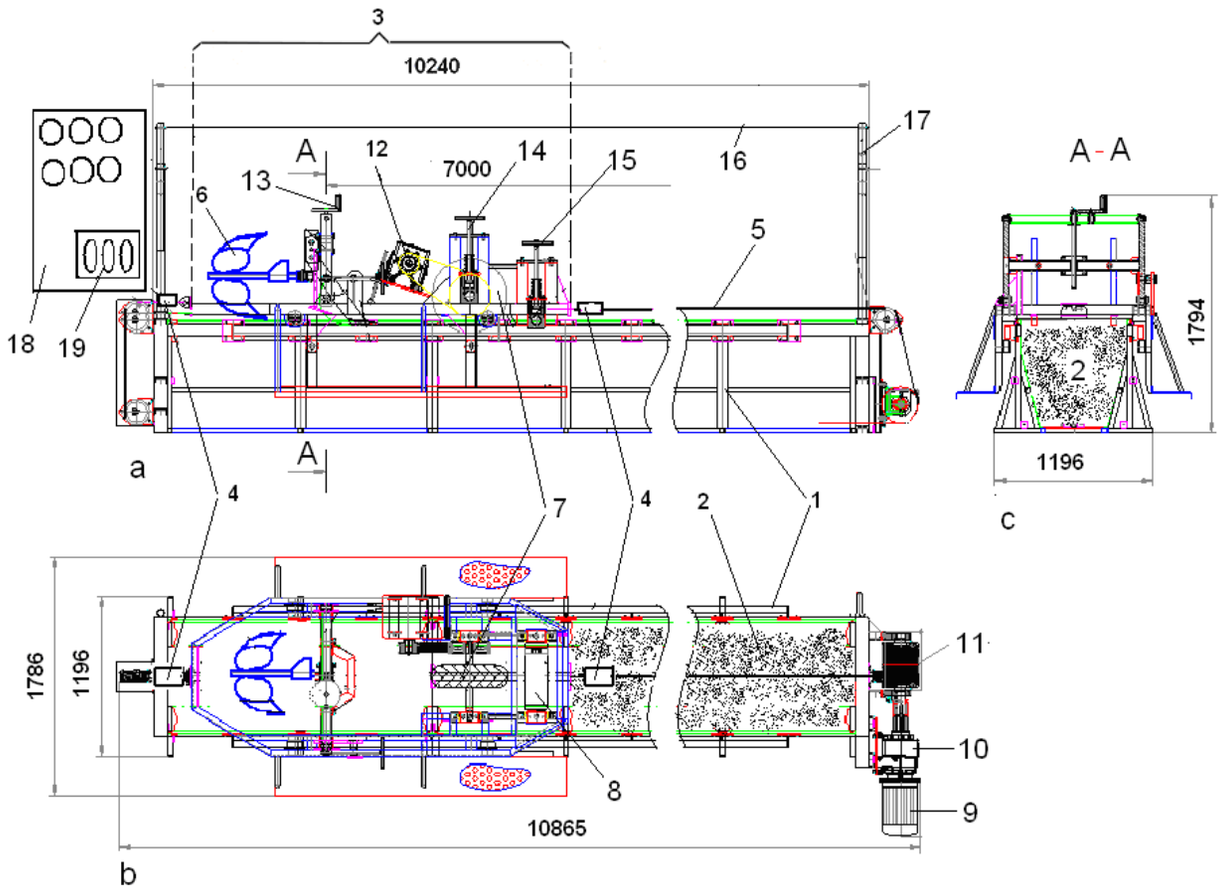

a – side view; *b – top view*; 1 – laboratory test rig frame; 2 – soil bin; 3 – carriage 4 – load cell; 5 – carriage cable trolley; 6 – active part (plow body); 7 – wheel with tire; 8 – drum for soil leveling and compaction; 9 – electric motor winch; 10 – cylindrical gear of the winch; 11 – traction cord reel; 12 – electric motor (and cylindrical gear) to drive the wheel with tire; 13 – screw mechanism for adjusting the working depth of the active body; 14 – screw mechanism for adjusting the vertical position of the wheel with tire; 15 – screw mechanism for adjusting the vertical position of the drum for soil leveling and compaction; 16 – steel cable to support the electric conductors; 17 – supporting pillars for the steel cable; 18 – electric power and control panel; 19 – controller to measure the traction force.

Figure 1. Laboratory test rig with soil channel for the study of the interaction between the active parts or agricultural wheels and the soil

The tests were aimed to evaluate the main operating parameters of the driving wheel test rig. The effects of the wheel speed, soil penetration resistance and wheel pushdown force over the carriage speed, wheel slip and wheel traction force were studied. The results obtained in these experiments are presented in Table 2.

Based on the experimental results it was concluded that wheel slip decreased when its speed was increased; in the meantime, the traction force decreased when its speed was increased.

As far as the soil resistance to penetration was concerned, it was concluded that its increase led to the increase of the wheel speed, because a more compact soil increases the adherence of the driving wheel; the increased adherence diminishes wheel slip, increases the carriage travel speed and also increases the traction force of the wheel.

(a) (b)

a – study of wheel – soil interaction; *b* –study of plough body – soil interaction.

Figure 2. Laboratory experiments in order to study of the interaction of tire wheel and active part with the soil

Working depth of plough body (mm)	Soil resistance to penetration (MPa)	Speed of plough body (m/s)	Traction force (N)	Specific power consumption (W/cm²)
100	0,2	0,75	705	2,65
		1,00	720	3,60
		1,25	735	4,59
	0,4	0,75	925	3,47
		1,00	940	4,70
		1,25	960	6,00
150	0,2	0,75	1055	2,64
		1,00	1070	3,57
		1,25	1080	4,50
	0,4	0,75	1380	3,45
		1,00	1400	4,67
		1,25	1420	5,92
200	0,2	0,75	1450	2,72
		1,00	1470	3,67
		1,25	1485	4,64
	0,4	0,75	1859	3,47
		1,00	1890	4,72
		1,25	1930	6,03

Table 1. Operating parameters of the laboratory test rig by modeling the plough body –soil interaction

Wheel speed (rot/min)	Soil resistance to penetration (MPa)	Down force over the wheel (N)	Speed of the trolley (m/s)	Driving wheel slip (%)	Traction force of the driving wheel (N)
20	0,2	500	0,50	17	230
		750	0,51	15	360
		1000	0,53	14	580
	0,4	500	0,51	15	290
		750	0,52	15	442
		1000	0,54	13	610
30	0,2	500	0,75	16	220
		750	0,76	15	350
		1000	0,79	12	570
	0,4	500	0,76	15	285
		750	0,77	14	438
		1000	0,79	12	600
40	0,2	500	0,99	15	220
		750	1,01	14	340
		1000	1,02	11	560
	0,4	500	1,01	14	280
		750	1,01	13	410
		1000	1,04	10	580

Table 2. Evaluation of the test rig's key operating parameters with motored wheel

Regarding the effect of the wheel down force, it was established that an increased force resulted in an increased wheel speed and, consequently, an increased travel speed of the carriage, due to the diminished wheel slip. The explanation is that an increased down force leads to a lower wheel slip, due to the higher wheel adherence; for the same reason, traction force increased when the wheel down force was increased.

Based on the experimental results precise correlations could be established between soil compaction and wheel slip, for a given vertical force acting over the wheel. In the same manner, the relationship between the vertical force and the traction force of the wheel was established, for a certain state of the soil.

4. Physical and mathematical modeling of the interaction between the active parts and soil

4.1. Introduction to numerical simulation

The finite volumes method (FVM) was used in order to model the interaction between the active parts of the agricultural equipment and soil. The equations specific to fluid flow are

partial derivatives equations. Moreover, these equations are non-linear and interconnected. Under these circumstances, solving the equations is possible only by the means of numerical methods [1, 5].

There are several types of numerical methods for solving the flow equations; the finite volumes method was preferred because it was considered the most appropriate for the simulation of flow and other soil related phenomena, for the particular case of soil-agricultural active part interaction. Within this method, the main stages for solving a problem regarding the soil-active part interaction are as follows:

- division of the soil model into control volumes (finite volumes), based on a computational mesh;
- integration of the equations for each control volume in order to obtain the algebraic equations which are characteristic to the unknowns of the problem;
- solving of the algebraic equations.

Regarding the first stage, the computational mesh may be "structured" (the geometrical elements are 2D triangles or 3D parallelepipeds) or "unstructured" (the geometrical elements are 2D quadrilaterals or 3D tetrahedrons).

The numerical simulation of the physical phenomena characteristic to fluid flow by the means of the CFD (computer fluid dynamics) method is entirely based on the fundamental laws that describe the flow of a fluid: mass conservation, momentum conservation, energy conservation [11].

Five methods may be used in order to solve the problems regarding the interaction between soil and the active parts: empirical and semi empirical methods, dimensional analysis, finite elements method (FEM), discrete elements method (DEM) and the neuronal networks method – ANN (Figure 3) [13].

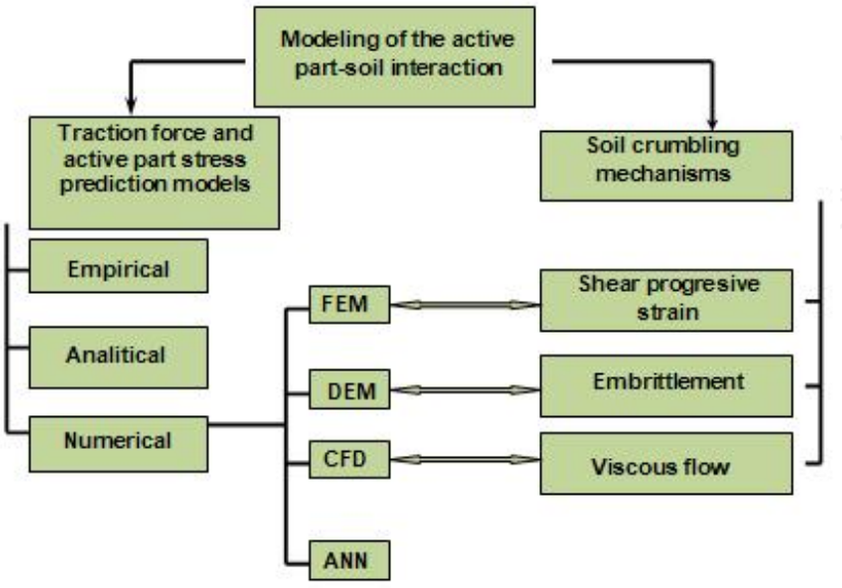

Figure 3. Methods for the numerical simulation of the active part-soil interaction

The mechanism of the active part-soil interaction may also be described using the rheological behavior of soil, taking into account its dynamic characteristics. The use of CFD method should take into account the dynamics of the active part-soil interaction, considering the irreversible deformations of the soil (see Figure 3) [21].

4.2. Case study regarding the CFD numerical simulation of the active part-soil interaction

The design criteria taken into account when building a tillage active part are traction resistance, the volume of the tilled soil and the overall energy requirements. The traction force depends on the pressure exerted by soil over the surface of the active part; soil pressure and its distribution are important items that should be considered when designing the size and shape of the active part.

The condition of the tilled soil depends on the soil's mechanical behavior and initial condition and on the characteristics of the active part. Soil is a complex material and its behavior is not yet fully understood. The complexity increases even further when taking into account different locations, with different climate conditions and different bulk densities. Several models for predicting the mechanical behavior of soil were considered over time, combining springs, dampers, slide-blocks, and from an elastic, plastic or viscous perspective. The behavior of most soils is non-linear and they can be considered as non-linear plastic or viscous-plastic materials. Thus, soil deformation may be described by a simple viscous-plastic model, the Bingham rheologic model.

The suggested shape of the winged share is a typical one (Figure 4a), but was adapted in order to increase its tillage performances. In the numerical simulation, the active part is mounted on a vertical holder (Figure 4b).

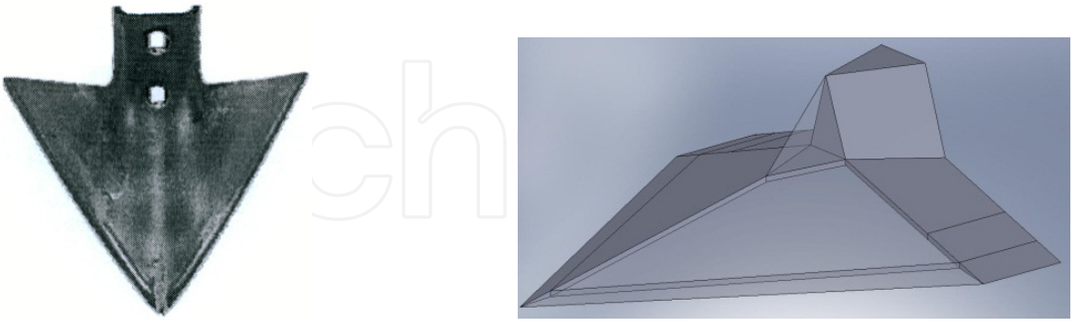

(a) (b)

a – existent; b - 3D model

Figure 4. Winged share

The numerical simulation assumes that the active part is stationary, while the viscous-elastic soil is flowing around the tillage tool (Figure 5).

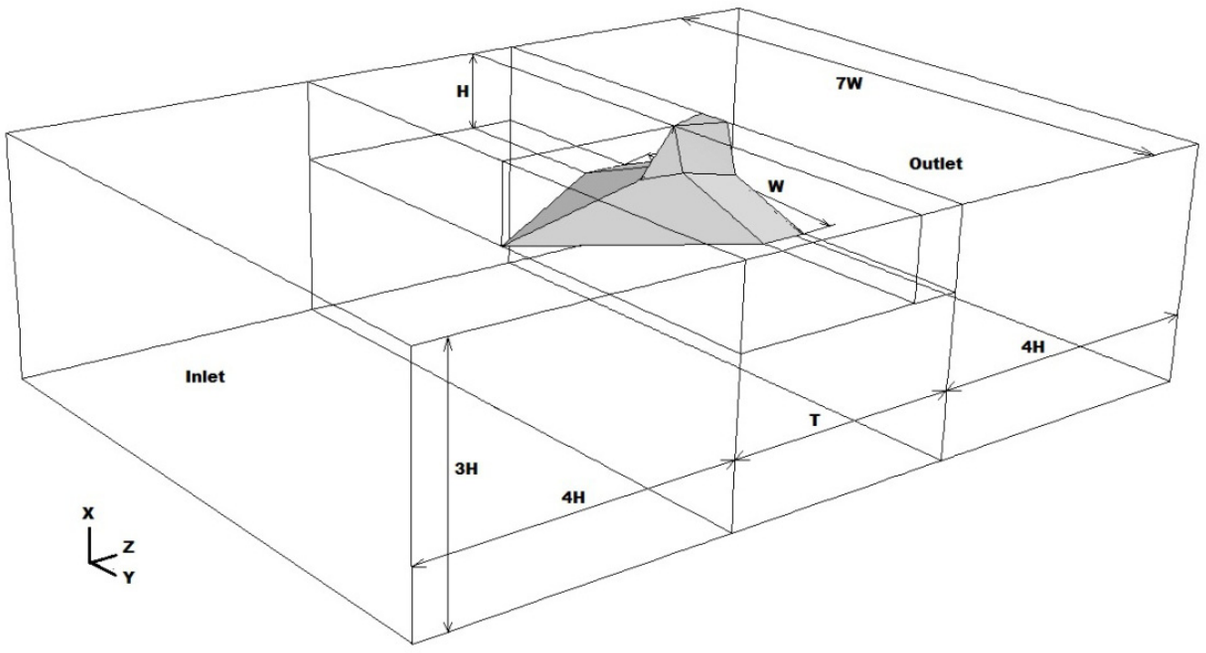

Figure 5. Schematics of the simulated domain (soil bin) and position of the active part

The active part acts as a resistance in the flow field and has the following dimensions: length T=140 mm, width W = 200 mm and height (equal to the working depth) H = 100 mm. The flow field is considered a parallelepiped with a length (8H+T) of 940 mm and a height (3H) of 300 mm. The sidewalls and the lower wall represent boundary conditions for the simulation field and their flow characteristics were neglected.

The CFD simulation showed that, for a soil bin seven times wider than the width of the active part, the wall effect of the bin disappears and an idealized flow pattern around the active part may be considered.

A mixed mesh was used in order to cover the computing domain, structured at the beginning and at the end of the bin and unstructured near the active part. At the tillage body level, the computational mesh was unstructured in the front and in the holder area, with a high density of the mesh, and structured behind the active part, with a lower mesh density (fig. 6). In order to cover the entire model 658000 elements were defined.

General and boundary conditions. The 3D CFD simulations were performed in isothermal conditions, for a loam-clay soil (38% clay, 32% silt and 30% sand – Figure 7), characteristic for the northeast area of Moldavia; these conditions imposed the use of the finite volumes method (FVM) for the CFD simulation.

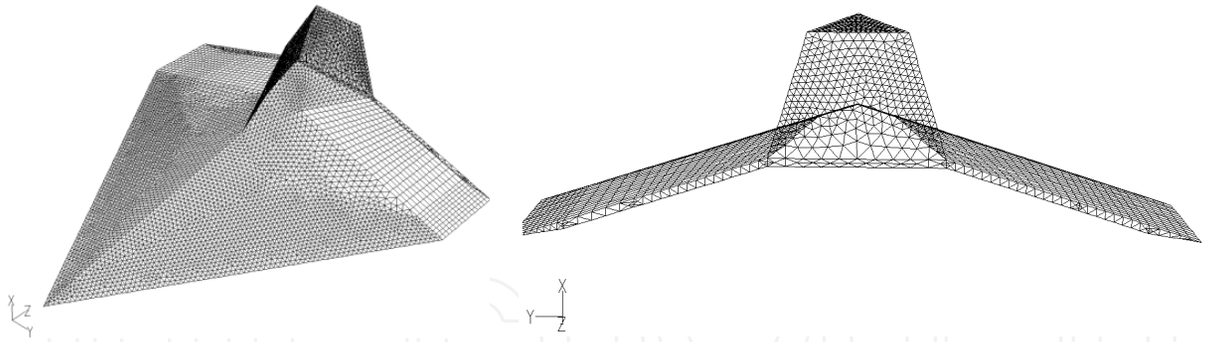

(a) (b)

a – view in the horizontal plane; b – view from behind in the vertical plane

Figure 6. Computational mesh and elements for the arrow type tillage body:

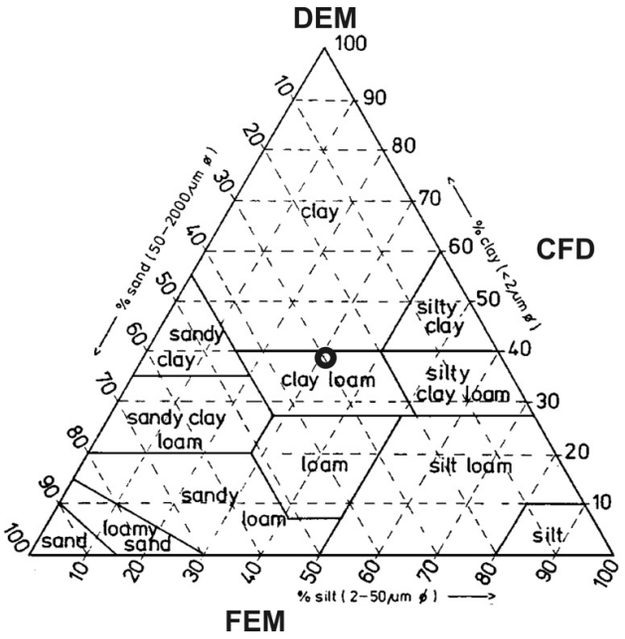

Figure 7. Soil classification according to sand, silt and clay content (texture triangle) and models for numerical simulation (**O** – present case study for soil with 38% clay, 32% silt and 30% sand) [15]

The viscous-plastic parameters of soil, such as the dynamic viscosity η and the shear yield stress τ_0, were evaluated at a constant speed, with a rheometer. Within the simulation the soil was considered at a humidity of 19% and a resistance to penetration of 400 kPa; other parameters taken into account were as follows: bulk density ρ = 1250 kg/m^3, dynamic viscosity η = 900 Pa·s and shear yield stress τ_0 = 12 kPa. The soil flow speed was w = 3 m/s, this being the traveling speed of the active part.

The following hypothesis were considered in the numerical simulation: a constant working depth of the tillage body; the active part was considered to be rigid; the soil flow was considered laminar and axisymetrical relative to the vertical section; 3D soil crumbling; the soil was considered an continuous, homogenous and anisotropic medium; soil behaves like a viscous-plastic Bingham material; the movement of the active part is considered with a

finite yield tension and the displacement of the active part is considered as interaction between the submerged body and the fluid; the interspace between the clods of soil is neglected and soil is considered to be incompressible; cracking of soil occurs when the shear yield for the soil in front of the active part is exceeded.

Generation of the model. The Navier-Stokes equations are the basic equations for solving any problem related to fluid flow, by taking into account the momentum conservation equations, applied to an element of volume. The assumption that soil is flowing as a fluid allows the analysis of different types of interactions between soil and the active part, like the soil pressure over the surface of the active part, the traction resistance etc.

According to the second law of Newton, the acceleration of the volume of fluid (elementary volume) is directly related to the force acting upon it by the means of the momentum conservation equation:

$$\rho \cdot \frac{du_i}{dt} = \rho \cdot g - \frac{\partial p}{\partial x_i} + \frac{\partial \tau_{ij}}{\partial x_j} \tag{1}$$

where d/dt is the full derivative, g is the acceleration of the gravity field (m/s^2), p is the hydrostatic pressure (Pa), τ_{ij} is the tensor of the shear stress (Pa), ρ is the density (kg/m^3), u_i is the travel speed (m/s) and x is the distance (m).

The full derivative of the fluid volume variation is a time and space dependent function:

$$\frac{du_i}{dt} = \frac{\partial u_i}{\partial t} + u_j \cdot \frac{\partial u_i}{\partial x_j} \tag{2}$$

Equation (2) shows that the gravitational force, the hydrostatic pressure and the viscous stress (hydrodynamic stress) balance the acceleration of the fluid element. According to this equation soil flowing may be processed taking into account several types of dynamic interactions between the active part and soil:

- forces produced by the speed and acceleration of the active part;
- soil pressure over the surface of the active part, taking into account the weight of soil;
- soil cracking due to the viscous-plastic deformations.

For the Bingham type of plastic fluids, the strain-stress relationship may be written as:

$$\tau_{ij} = \sigma_i = 2 \cdot \mu \cdot \frac{\partial u}{\partial x} \tag{3}$$

$$\tau_{ij} = \tau_y + \mu \cdot \left(\frac{\partial u_i}{\partial x_j} + \frac{\partial u_j}{\partial x_i} \right), \text{for} \quad \left| \tau_{ij} \right| > \tau_y \tag{4}$$

$$\gamma = 0, \text{for} \quad \left| \tau_{ij} \right| \le \tau_y \tag{5}$$

where $\tau_y = \tau_0$ is the yield stress (Pa), $\mu=\eta$ is the plastic or dynamic viscosity ((Pa·s), γ is the shearing speed (u/h being the flowing speed gradient) (s^{-1}) and h is the thickness of the sheared layer (m).

In a cartesian system of coordinates (x, y, z) the x component of the equation (1) may be expressed, based on the equations (2 - 4), in the form:

$$\rho \cdot \left(\frac{\partial u}{\partial t} + u \cdot \frac{\partial u}{\partial x} + v \cdot \frac{\partial u}{\partial y} + w \cdot \frac{\partial u}{\partial z} \right) = -\frac{\partial p}{\partial x} + \frac{\partial}{\partial x}\sigma_x + \frac{\partial}{\partial y}\tau_{xy} + \frac{\partial}{\partial z}\tau_{xz} \tag{6}$$

where τ_{xy} is the shear stress in the xy plane (Pa), τ_{xz} is the shear stress in the xz plane (Pa), σ_x is the normal stress (Pa) and u, v, w are characteristic coefficients of the x, y, z axes.

In order to satisfy the assumption that the viscous-plastic fluid is homogenous and isotropic, the simulation assumes that the yield stress is not dependent on the position or the orientation of the fluid particles.

In the tillage process, the active body has to overcome soil rigidity and cracking appears only when the tangential stress exceeds the yield stress. When the applied force exceeds the yield stress limit, soil flows as a viscous-plastic fluid, due to shear cracking.

The traction force is equal to or higher than the drag force; in the present simulation the active part is considered to be submerged into soil; hence, the drag force F is given by the relation:

$$F = \frac{1}{2} \cdot C_D \cdot \rho \cdot u_z^{\,2} \cdot A \tag{7}$$

where C_D is the drag coefficient, ρ is the density of soil, (kg/m^3); u_z is the speed along the z axis (m/s), A is the characteristic area of the active part (m^2).

The drag coefficient has two components: the drag coefficient due to pressure C_{Dp} and the drag coefficient due to friction, C_{Df}:

$$C_D = C_{Dp} + C_{Df} \tag{8}$$

The weight of each drag component (pressure and friction) depends on the geometrical shape of the active part. The aim of the simulation is to obtain the geometrical shape leading to a minimum drag of the active part with.

A value of 10^{-4} was considered as the convergence criterion for each iteration and for each of the equations of the flowing process. A relaxation coefficient of 0.3 was chosen in order to maintain a stable convergence (a higher relaxation coefficient increases the convergence time). The results of the simulations were than interpreted considering that the active part is traveling at a constant speed.

Simulations were performed over three types of active parts, with the same geometrical shape, but with different angles between the cutting edges: $2\gamma = 60^0$; $2\gamma = 66^0$; $2\gamma = 70^0$.

Pressure distribution over the surface of the arrow type active body depends on the position of the cutting surfaces and on the characteristics of the soil. The simulations show that the maximum pressure is recorded on the cutting edges.

Table 3 presents the effect of the 2γ angle over the variation of the average normal pressure, for the same type of soil. The distribution of the normal pressure on the surface of the active part is shown in Figure 8.

2γ (degrees)	60	66	70
Average pressure (kPa)	4.4 ... 45.2	4.5 ... 53.5	4.45 ... 53.35

Table 3. Variation of the average normal pressure along the cutting edges

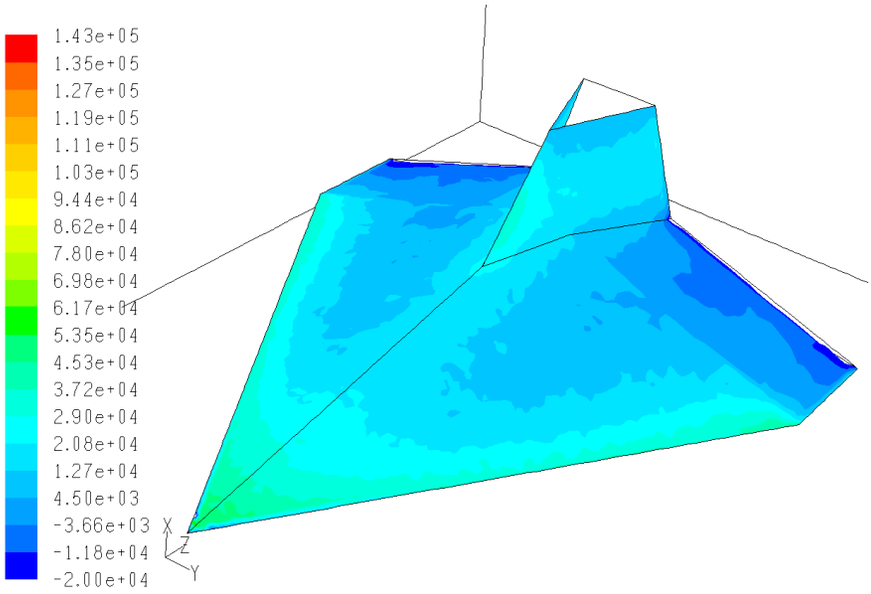

Figure 8. Distribution of the normal pressure (Pa) on the surface of the active part

As previously mentioned, drag has two components, one due to pressure and the other due to friction; therefore, the same two components (pressure and viscosity) are present within the traction force (Table 4).

The tangential stress distribution over the surface of the active part (the viscosity or friction component) reaches a maximum on the cutting edges and diminishes towards the inner part of the active body (Figure 9).

Figure 10 presents the variation of the soil speed; the soil is disturbed in front of the active body and the distribution pattern of the flowing speed clearly indicates the region where the cracks appear. Speed variation along the longitudinal (z) axis presents two distinct flowing regions (Figure 10b): one corresponds to the viscous-plastic flow, in the vicinity of the active part, when the tangent stress exceeds the yield point, and the second one corresponds to the area where the tangent stress does not exceed the yield point, while the second implies a flowing resistance ("solid flow"), when the tangent stress does not exceed the yield point; the soil is an elastic state.

Because the simulation assumes that soil flows while the active part is considered stationary, the soil speed on its surface is zero; speed is also zero in the contact area with the soil bin walls. Moving away from the surface of the active part, the speed increases; as a result, near the active part, the tangent stress records very high levels and the yield point is exceeded, leading to the formation of cracks and to a viscous-plastic strain.

Region	Force due to static pressure (N)			Force due to viscosity (N)			Overall force (N)		
	$2\gamma = 60^0$	$2\gamma = 66^0$	$2\gamma = 70^0$	$2\gamma = 60^0$	$2\gamma = 66^0$	$2\gamma = 70^0$	$2\gamma = 60^0$	$2\gamma = 66^0$	$2\gamma = 70^0$
Surface of the active part	86.1	95.6	102.4	415.6	520.4	642.3	501.7	616.0	744.7
Surface of the active part holder	40.07	36.3	39.1	46.2	42.5	32.8	86.27	78.8	71.9
TOTAL	126.17	131.9	141.5	461.8	562.9	675.1	587.97	694.8	816.6

Table 4. Traction force for the winged share type active part

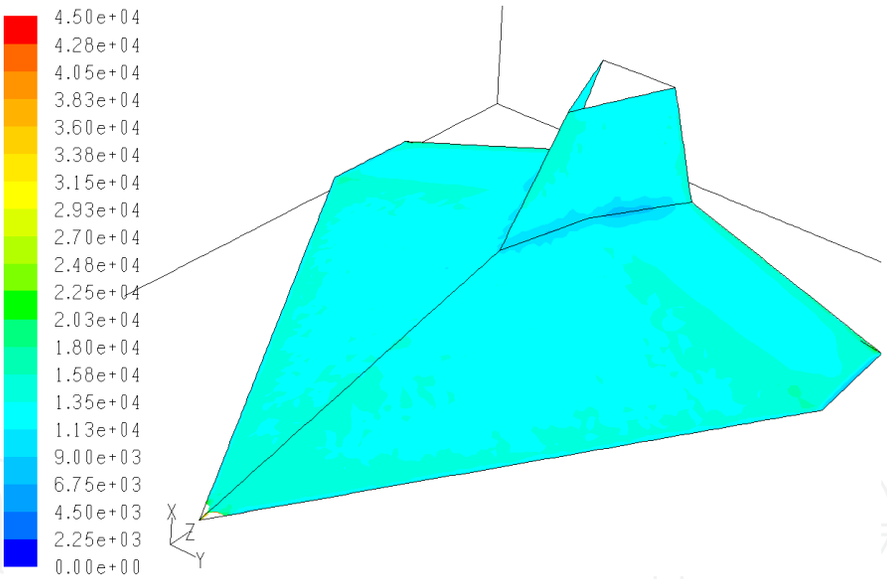

Figure 9. Distribution of the tangential stress (Pa)

5. Physical and mathematical modeling of the tire wheel-soil interaction

5.1. Simulation principles applied within the finite elements method (FEM)

The finite elements method (FEM) is used in order to study the bodies with a complex shape, providing numerical solutions for different physical characteristics when analytical solutions are impossible or very difficult to obtain. The finite element analysis (FEA) is used within this method [6].

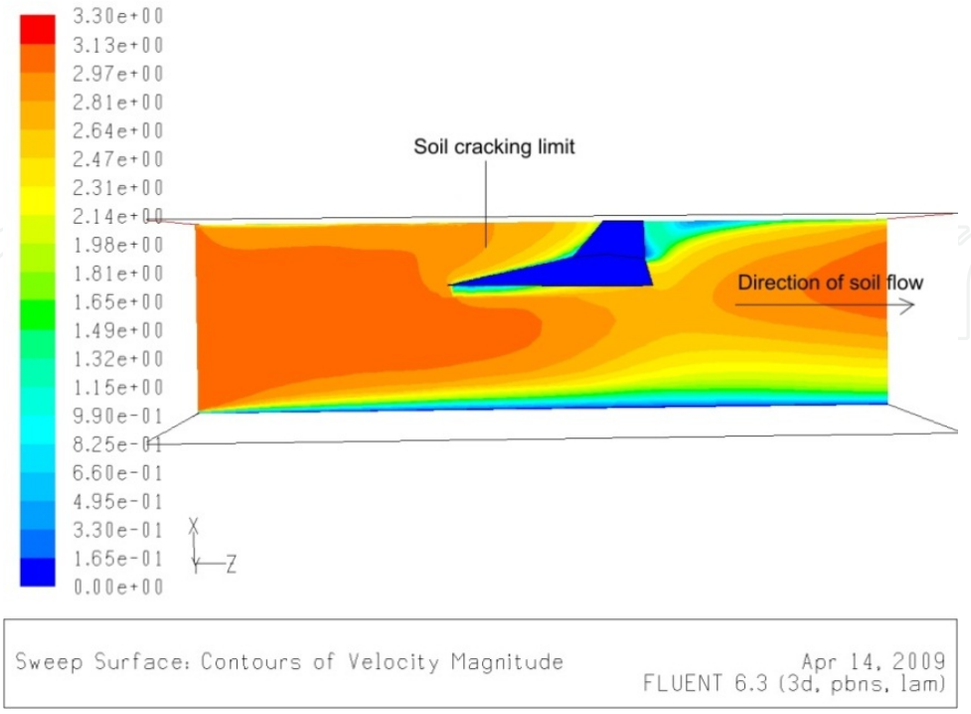

(a)

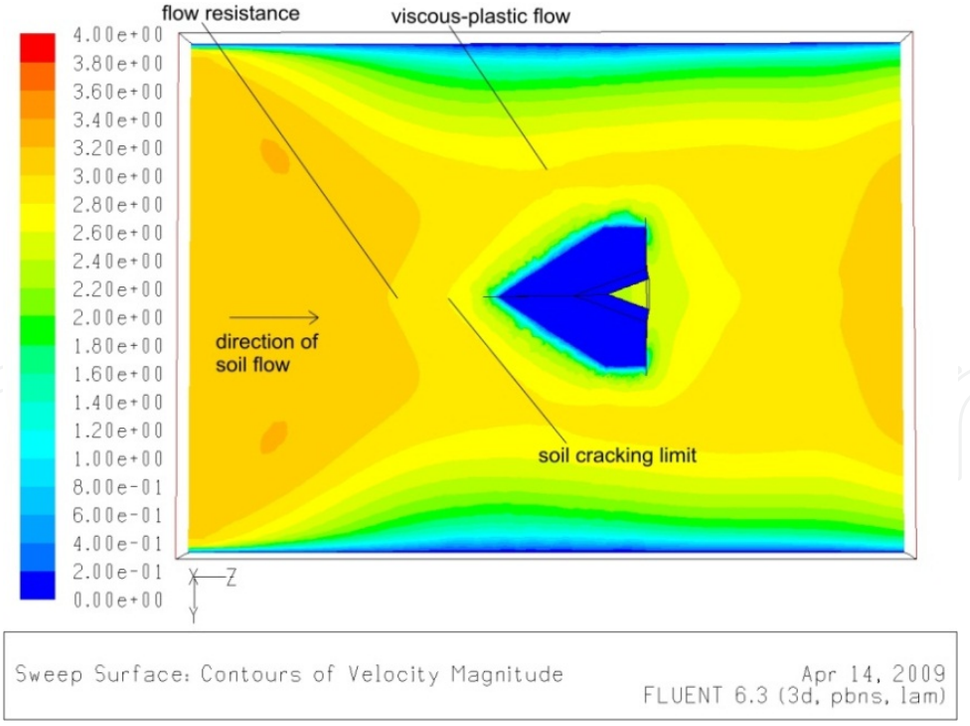

(b)

Figure 10. Soil speed profile (m/s) in the longitudinal vertical plane XOZ (a) and horizontal plane YOZ (b), for $2\gamma=66^0$.

The finite elements method is based on the principle of the overall potential energy, which states that a structure or a body is deformed or displaced in a position that minimizes the potential energy (overall potential). This is in correspondence with the second law of thermodynamics, which states that the entropy of an isolated system can only increase towards a maximum value, meaning that the capacity to produce mechanical work can only decrease.

The principle of the minimum potential energy has many applications in the mechanics of the solid bodies and in the analysis of structures. In these cases, the principle of the minimum overall potential is a special case of the principle of virtual mechanical work applied to systems being under the action of conservative forces. The principle of the virtual mechanical work states that the virtual mechanical work of the exterior forces is equal and opposed to the virtual mechanical work of the interior forces (normal stress, shear stress, torsion and bending stress). It is assumed that forces and stresses remain constant and only the variations of strains are taken into account; only the strains that satisfy the internal compatibility of the body and the boundary conditions (resulting from the connections to other bodies) are accepted.

The finite elements method was imposed by the need to solve complex problems regarding the mechanics of deformable bodies. The method may be also applied to the problems referring to the flow of fluids, heat transfer, magnetic fields etc. [16].

5.2. Numerical simulation of the wheel-soil interaction

The first applications of the finite elements method – FEM – were aimed to simulate the linear elastic materials, but now this method is also used for non-linear, non –elastic materials like soil. Unlike metals, soil has a very low tensile strength; when compressed, the deformation reaches the plastic domain and soil has the tendency to remain in the deformed state. The wheel-soil interaction takes place in the non-linear domain, which means that a greater number of finite elements should be used in the simulation; the computation time increases accordingly.

In agriculture, the 3D simulations of the wheel-soil interaction aim to produce solutions leading to the limitation of soil compaction. A certain number of tests must be performed, with different types of soils and the results of the tests are than used in the numerical simulation in order to obtain a realistic prediction. These results allow the reduction of the design costs and the design time of the agricultural equipment according to the principles of sustainable agriculture.

The 3D numerical simulation based on FEM assumes some simplification hypothesis: the wheel is considered to be under the action of a dynamic vertical load; the wheel is assumed rigid; the number of vertices is limited by the computing power available; the soil characteristics are estimated ones, due to its heterogeneous characteristics.

Description of the model. The FEM software ABAQUS was used in order to build the 3D model for the analysis of soil compaction. Taking into account the complexity of the model the "explicit" version of the software was used, instead of the "standard" one; this approach allows the further development of the model by considering a deformable wheel instead of a rigid one.

The model is composed of two distinct 3D elements: a portion of the soil bin and the rigid wheel. In order to diminish the computation time, a vertical plane of symmetry, parallel to the direction of travel, was considered, dividing the contact patch into two symmetrical portions; simulation was therefore performed on only one half of the 3D soil-wheel model. The cartesian reference system was defined as follows (Figure 11): the negative z axis was considered to be along the travel direction, the positive x axis was perpendicular to the soil surface and the y axis was perpendicular to the travel direction and parallel to the wheel axis.

Static soil model. The 3D model of the soil was divided into five sections (Figure 11), each with a different density of the dicretization mesh; the contact surfaces between the sections were considered to be bound to each other. A higher density of the mesh was used for the wheel-soil contact area, on a depth of 0.05 m; a lower mesh density was used for the rest of the model.

The finite soil elements are 3D solid parallelepipeds, with 8 vertices and only three degrees of freedom, corresponding to the translations along the directions x, y and z. The computation time is thus significantly reduced and the stability of the model is increased.

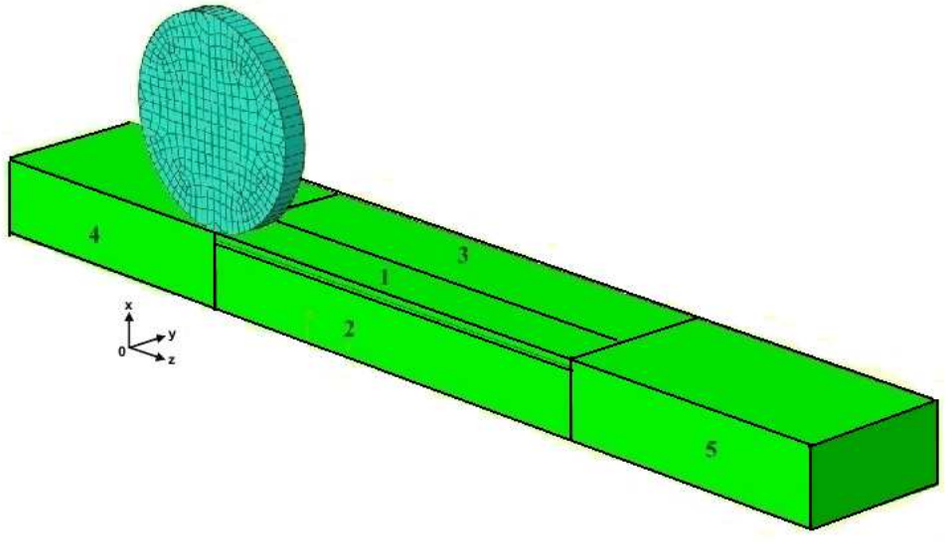

Figure 11. The 3D wheel-soil model

In order to extend the length and width of the simulation model to infinity, infinite solid elements were attached; they were considered 3D parallelepipeds, with eight vertices and one infinite face. These elements were used for the elastic linear deformation domain and were attached to the boundaries of the solid element.

The strain-stress curve was considered to be composed of linear portions, as shown in Table 5. The physical and mechanical properties of soil were those presented by Block [3]. The density of soil was $\rho = 1255.2$ kg/m^3, the modulus of elasticity was E = 0.3262 MPa and the initial Poisson's ratio was assumed to be $\nu = 0.3$.

Yield strength (MPa)	Volumetric strain	Yield strength (MPa)	Volumetric strain
0	0	0.08	0.149679
0.005	0.014661	0.09	0.160028
0.01	0.028334	0.10	0.169280
0.02	0.053024	0.12	0.185036
0.03	0.074619	0.16	0.208422
0.04	0.093572	0.21	0.228045
0.05	0.110262	0.29	0.248232
0.06	0.125006	0.40	0.266976
0.07	0.138069	0.50	0.280999

Table 5. The strain/stress curve

The infinite elements use the same material properties; the initial elasticity modulus increases with compaction, due to the increase of the rigidity. The Poisson's ratio is modified during the simulation. The soil was modeled with ABAQUS/Explicit as "cap plasticity" and optionally as rigid "cap hardening". These options allow the plastic strain to start from a prescribed level, which is included in the Drucker-Prager rigidity model. Each layer of soil has an initial volumetric strain corresponding to the hydrostatic pressure induced by the weight of the above layers. An initial compaction of the soil was taken into account. The "cap plasticity" option imposes the definition of three supplementary parameters (for the sandy clay soil): the cohesion coefficient c = 350 Pa, the friction angle $\beta = 57.8^0$ and the "cap eccentricity" parameter R = 0.0005. The values "cap plasticity" and "cap eccentricity" were evaluated in the process of optimizing the Block model.

The yield strength due to the hydrostatic pressure was limited to values between 0.005 and 0.5 MPa.

Dynamic model of the rigid wheel. The rigid wheel was considered a cylinder, composed of 3D discrete rigid elements. The simulation in ABAQUS/Explicit was performed for two types of loads: concentrated load, applied in the center of the wheel, and distributed load, applied on the circumference of the wheel.

Boundary conditions. Specific boundary and loading conditions were considered within the simulation. The boundary conditions were defined for the soil model, for the rigid wheel model and for the wheel-soil interaction. The base of the soil model was restrained from moving along the x, y and z axis; the initial condition was defined considering an untilled soil with a certain degree of compaction. No constraint was defined for the soil-wheel interface.

Two constraints were defined for the wheel, referring to the acceleration of gravity and wheel rotation.

The interaction between wheel and soil was simulated by the means of two surfaces, corresponding to the cylindrical surface of the wheel and exterior soil surface. Thus, the wheel gradually loaded the soil. No slip was assumed during wheel rolling.

Loading conditions. The maximum wheel load of 5.8 kNa was reached in 12 time steps. The duration of each of the first five steps was set to one second; during these steps, each element was progressively loaded from zero to 9.81 m/s^2. After the first five seconds, the wheel acceleration was constant. During the following seven time steps (each with a duration of two seconds), the rotation speed of the wheel was increased from zero to 0.244 rad/s (16.74 cm/s travel speed).

Simulation results. The simulation was aimed to evaluate soil compaction, the indentation depth of the wheel and the normal stress. The 3D simulation emphasized the residual soil stress, leading to soil compaction and destruction of the structure in the contact area.

Three locations were chosen for the evaluation of the normal stress. The first one was placed at a depth of 0.3 m under the center of the wheel-soil contact patch, the second one was placed at a depth of 0.3 m under the outer edge of the wheel (y = 0,16 m) and the third one was placed at 0.15 m beneath the center of the contact patch. Table 6 presents the values of the normal stress, after 12 seconds, in the above-mentioned locations.

Wheel load (kN)	Indentation depth (m)	Location	Normal stress (kPa)
5.8	0.101	1	14.5
		2	7.0
		3	17.0

Table 6. Simulation results

6. The effect of tillage operations and of the agricultural traffic over soil

6.1. Materials and methods

The task of tillage is to prepare soils for productive use; it is performed in order to bring the seedlings into the soil and procure for them a good environment for further development. Tillage operations may have negative effects over the physical and mechanical properties of soil, over plant development and agricultural yield.

The experiments were aimed to investigate the effect of soil tillage technologies and soil compaction over the penetration resistance, apparent soil density, weighted average diameter of the soil's structural elements and water stability of the aggregates.

The experiments were performed on a mezocalcaric cambic chernozem, with a clay-loam texture and eastern exposure.

Experimental variants. The experimental variants are summarized in table 7. Soil compaction was achieved before tillage, by running the Valtra T190 tractor once over the field (compacted once) or twice (compacted twice), at a travel speed of 2.5 km/h.

The experimental field was seeded with the Glosa variety of autumn wheat (approved in Hungary, in 2005); the row spacing was 125 mm, and the seeding depth was 5 cm.

Agricultural equipments and operations	Soil compaction	Experimental variants
Plowing with T190[1] + Opal 140 Secondary tillage with U-650[2] + GD-3,2 Sowing with U-650 + SUP-29	non-compacted	V_1 - control
	compacted once	V_2
	compacted twice	V_3
Plowing with T190 + Opal 140 Secondary tillage with T190 – BS 400 A Sowing with U-650 + SUP-29	non-compacted	V_4
	compacted once	V_5
	compacted twice	V_6
Direct sowing, in untilled soil, with T190 + MCR-2,5	non-compacted	V_7
	compacted once	V_8
	compacted twice	V_9
Loosening of the unplough soil (14 cm), seedbed preparation and sowing with T190+OA+AGPS-24DR[3]	non-compacted	V_{10}
	compacted once	V_{11}
	compacted twice	V_{12}
Plowing with T190 + Opal 140 Seedbed preparation and sowing with T190+ AGPS-24DR[4]	non-compacted	V_{13}
	compacted once	V_{14}
	compacted twice	V_{15}

Table 7. Experimental variants

Evaluated soil degradation indices

The specific resistance to penetration was evaluated ten days after sowing, using the Eijelkamp (Holland) static penetrometer. The specific penetration resistance is ranked as:

- very low (lower than 1.08 MPa);
- low (1.08 – 2.45 MPa);
- average (2.45 – 4.9 MPa);
- high (4.9 – 9.81 MPa).

A specific penetration resistance lower than 2.45 MPa allows the normal development of plant roots; for values between 2.45 and 9.81 MPa the development of roots is partially limited; for values higher that 9.81 MPa, the roots development is stalled.

[1] T190 – Valtra tractor, 190 HP.
[2] U650 – Romanian tractor, 65 HP.
[3] OA+AGPS-24DR is composed of a rotary harrow and a seeder; OA are winged type shares mounted in the front of the rotary harrow.
[4] AGPS-24DR is composed of a rotary harrow and a seeder.

Bulk density of soil

In order to evaluate this index untilled soil samples were taken ten days after sowing, from the following depths: 0 – 10 cm, 10 – 20 cm, 20 – 30 cm and 30 – 40 cm.

For the clay-loam soil, the bulk density is ranked as:

- extremely low (loosened soil) – under 1.05 g/cm^3;
- very low (moderately loosened soil) - 1.05 – 1.18 g/cm^3;
- low (slightly loosened soil) - 1.19 – 1.31 g/cm^3;
- average (slightly compacted soil) - 1.32 – 1.45 g/cm^3;
- high (moderately compacted soil) - 1.46 – 1.58 g/cm^3;
- very high (very compacted soil) – over 1.58 g/cm^3.

The weighted average diameter of the structural elements. The structure of the arable layer is characterized by the grain size distribution. A device with sieves of different sizes (10; 5; 3; 2; 1; 0,5 and 0.25 mm) is used to evaluate this index, by sieving the soil samples.

The weighted average diameter is calculated with the formula:

$$WAD = \frac{\sum(p_i \cdot d_i)}{100}, \text{mm}$$

where p_i is the share of each size fraction [%] and d_i is the mean diameter of each size fraction [mm].

The Tiulin- Erikson method ranks the weighted average diameter as:

- very good (WAD = 2 – 5 mm);
- good (WAD = 1 -2 mm and 5 – 7 mm);
- acceptable (WAD = 0.25 – 1 and 7 – 10 mm);
- poor (WAD under 0.25 and over 10 mm).

Water stability of the aggregates. Represents the property of soil aggregates to withstand the dispersion action of water. The soil sample (20 g) is dispersed, entrained and sieved in a flow of water; in the Tiulin-Erikson apparatus, the sieves have apertures of 0.25; 0.5; 1; 2; 3; 5 mm.

The aggregates retained on each sieve are weighted and the I_1 water stability index is calculated with the formula:

$$I_1 = \frac{I + II + III}{IV + V}$$

where I is the percent of aggregates bigger than 5 mm, II is the percent of aggregates of 3 – 5 mm, III is the percent of aggregates of 2 – 3 mm, IV is the percent of aggregates with 1 – 2 mm and V is the percent of aggregates of 0.5 - 1 mm. According to I_1, the water stability of aggregates is ranked as follows:

- 3.00 – 5.00 – very good structure;
- 0.61 – 3.00 – good structure;
- 0.30 – 0.61 – medium structure;
- 0.18 – 0.30 – poor structure;
- lower than 0.18 – bad structure.

6.2. Results and discussions regarding the effect of soil tillage technologies and soil compaction over the physical and mechanical properties of soil

The experiments were aimed to investigate the effect of soil tillage technologies and soil compaction on the penetration resistance, apparent soil density, weighted average diameter of the soil's structural elements and water stability of the aggregates.

Resistance to penetration. The experiments were performed over three agricultural years (2008/2009, 2009/2010, 2010/2011) and the penetration resistance was evaluated for four depths (0 – 10 cm, 10 – 20 cm, 20 – 30 cm, 30 – 40 cm); the averaged values for the agricultural years and 0 – 40 cm depth are presented in table 8.

The results show very low values of the penetration resistance (0.438); according to the agro technical requirements, values lower than 1.08 MPa are considered "very low" and roots may develop normally.

Based on the penetration resistance, the five variants referring to the non-compacted soil were ranked as follows: V_{13} (the best), V_4, V_1, V_{10} and V_7 (the worst). Because soil was not compacted, these values were considered as reference in order to establish the effect of the tillage equipments.

Compaction	Penetration resistance [MPa]				
Non-compacted	V_1	V_4	V_7	V_{10}	V_{13}
	0.247	0.236	0.286	0.260	0.215
Compacted once	V_2	V_5	V_8	V_{11}	V_{14},
	0.326	0.315	0.356	0.347	0.306
Compacted twice	V_3	V_6	V_9	V_{12}	V_{15}
	0.406	0.390	0.438	0.410	0.387

Table 8. The effect of the tillage technologies over the resistance to penetration

The experimental data show that the compaction of the soil (once and respectively twice) has significantly increased the penetration resistance.

The lowest values of the penetration resistance were recorded for the variants V_{13} (non-compacted soil), V_{14} (compacted once) and V_{15} (compacted twice), when plowing was performed with the T190 + Opal 140 unit and the seedbed preparation and sowing were performed with the T190+ AGPS-24DR equipment.

Low values of the penetration resistance were also recorded for the variants V_4 (non-compacted), V_5 (compacted once) and V_6 (compacted twice), when the same equipment was used for plowing (T190 + Opal 140) and the BS 400 combined equipment was used for seedbed preparation.

The increase of the penetration resistance (compared to variants V_{13}, V_{14} and V_{15}) was due to the presence of cage rollers and cross kill roller (mounted in the back of the equipment).

For the following variants (V_{10}, V_{11} and V_{12}), classical plowing was replaced by a tillage operation performed with the OA + AGPS-24DR complex equipment; the soil was loosened over a depth of 15 cm by the OA winged type shares, mounted in front of the rotary harrow. As a result, the penetration resistance increased significantly.

Strip tillage was performed for the variants V_7, V_8 and V_9, by the means of the MCR 2.5 combined equipment; in this case, isolated bands of soil were tilled (only one third of the equipment's working width), to a depth of 8 cm. This solution led to the higher values of the penetration resistance.

Soil bulk density. Table 9 presents the experimental results referring to the bulk density of soil. The values are averaged ones, for three agricultural years and four depths.

Compaction	Bulk density [g/cm^3]				
Non-compacted	V_1	V_4	V_7	V_{10}	V_{13}
	1.31	1.28	1.33	1.32	1.26
Compacted once	V_2	V_5	V_8	V_{11}	V_{14},
	1.42	1.40	1.45	1.43	1.39
Compacted twice	V_3	V_6	V_9	V_{12}	V_{15}
	1.51	1.49	1.58	1.54	1.46

Table 9. Effect of tillage technologies over the bulk density of soil

For variants V_{13}, V_4 and V_1 (non-compacted soil) the bulk density was low (poorly loosened soil), while average values were recorded for variants V_{10} and V_7 (slightly compacted soil). Average values were also recorded for all the "compacted once" variants (slightly compacted soil); the high values of the bulk density reported for the "compacted twice" variants ranked them as "moderately compacted".

Taking into account that lower values of the bulk density are desirable, the "non-compacted" variants were ranked as follows: V_{13} (the best), V_4, V_1, V_{10} and V_7 (the worst).

The experimental results showed that bulk density increases when soil compaction increases. The "compacted once" and "compacted twice" variants were ranked exactly in the same order as the "non-compacted" variants, in terms of bulk density, because their ranking is only due to the type of tillage equipment. Moreover, the same ranking was recorded in terms of penetration resistance, because the both indices are characterizing the compaction state of soil and the increase of one index implies the increase of the other one, too.

Average weighted diameter (WAD) of the structure elements. Table 10 presents the experimental results referring to the average weighted diameter of the soil's structure elements. The values are averaged ones, for three agricultural years and three depths.

Compaction	Weighted average diameter [mm]				
Non-compacted	V_1	V_4	V_7	V_{10}	V_{13}
	3,70	3,68	3,56	3,40	3,35
Compacted once	V_2	V_5	V_8	V_{11}	V_{14},
	3,05	3,09	3,34	3,20	3,19
Compacted twice	V_3	V_6	V_9	V_{12}	V_{15}
	2,84	2,88	3,29	2,97	2,90

Table 10. Effect of tillage technologies over the weighted average diameter.

WAD varied between narrow limits – 2.845 mm to 3.702 mm. The results include the weighted average diameter in the 2 – 5 mm class (very good), for all the variants. Within this class, the best weighted average diameter is the one that is closest to 3.5 mm.

According to this index, the "non-compacted" variants were ranked as follows: V_7 (the best), V_{10}, V_{13}, V_4 and V_1 (the worst).

The "compacted once" and "compacted twice" variants were ranked exactly in the same order as the "non-compacted" variants, in terms of weighted average diameter, due to the facts previously mentioned.

Increasing the compaction of soil resulted in a marked destruction process, the weighted average diameter being diminished.

Variant V_7 was ranked the first due to the limited tillage process, during which the soil aggregates were less affected; when using the MCR-2.5 equipment, only isolated bands of soil were tilled (on one third of the equipment's working width), to a lower depth of 8 cm and thus the structural elements are preserved.

Variant V_{10} was ranked second because soil plowing was replaced by loosening to a depth of 15 cm. The fact that seedbed preparation and sowing were performed simultaneously also contributed to the preservation of the soil's structure. In the same time, the more intense tillage (performed by the OA winged type shares and the rotary harrow) applied within this variant led to lower weighted average diameters of the aggregates.

In the case of variant V_{13}, which was ranked the third, classic moldboard plowing led to the destruction of the structure elements; seedbed preparation by the means of the FRB-3 rotary harrow (part of the AGPS-24DR complex equipment) also contributed to the diminishing of the aggregates' diameter.

Variant V_4 was ranked the fourth due to conventional plowing, followed by the secondary tillage performed with the BS 400A combined equipment. The great number of tillage equipments within its structure, of which three are rollers, had an unfavorable effect over the soil structure.

Water stability of the aggregates. Table 11 presents the experimental results referring to the water stability of the soil's aggregates. The values are averaged ones, for three agricultural years and three depths.

Compaction	I_1 index				
Non-compacted	V_1	V_4	V_7	V_{10}	V_{13}
	3.60	3.61	4.18	3.70	3.68
Compacted once	V_2	V_5	V_8	V_{11}	V_{14},
	2.84	2.96	3.43	3.18	3.02
Compacted twice	V_3	V_6	V_9	V_{12}	V_{15}
	2.64	2.68	2.93	2.77	2.78

Table 11. Effect of tillage technologies over the water stability of aggregates (I_1 index)

The values of the I_1 index were comprised between 2.64 and 4.18, which means that two classes were included: very good structure (3.00 – 5.00) and good structure (0.61 – 3.00). The higher the I_1 index, the better the soil structure. Within the 3.00 – 5.00 class, the best soil structure is the one that is closest to 4.00.

For the "non-compacted" variants, their ranking was as follows: V_7 (first place), V_{10}, V_{13}, V_4 and V_1 (last place).

The "compacted once" and "compacted twice" variants were ranked exactly in the same order as the "non-compacted" variants in terms of weighted average diameter, due to the previously mentioned facts regarding soil compaction.

The ranking of the variants respected the same order as in the case of the weighted average diameter.

It should be mentioned that an increased soil compaction results in a lower I_1 index; this tendency becomes more important when passing from the "non-compacted" variants to the "compacted once" variants.

6.3. Results regarding the effect of tillage technologies and soil compaction over the yield of seed for the autumn wheat crop.

The experimental variants are the ones already presented in the discussion referring to the effect of soil tillage and compaction over the physical and mechanical properties of soil.

The results regarding the seed yield are presented in table 12, being the averaged values for three agricultural years.

The experimental variants on the first five places ("non-compacted" soil) are ranked as follows: V_{10} (best), V_7, V_{13}, V_4 and V_1 (5^{th} place).

The next five places belong to the "compacted once" variants, in the following order: V_{11} (6^{th} place), V_8, V_{14}, V_5 and V_2 (10^{th} place).

The last five places were taken by the "compacted twice" variants: V_{12} (11^{th} place), V_9, V_{15}, V_6 and V_3 (15^{th} place).

As far as the tillage and sowing technology are concerned, the order is similar for the "non-compacted", "compacted once" and "compacted twice" variants, as only the type of tillage and sowing equipment affected ranking.

It should be noticed that yield decreases when soil compaction increases; this tendency is more significant when passing from the "non-compacted" variants to the "compacted once" variants.

Tillage and sowing equipments	Compaction	Experimental variants	Seed yield, kg/ha
Valtra T190 + Opal 140; U-650 + GD-3,2; U-650 + SUP-29	non-compacted	$V_{1 - witness}$	5765
	compacted once	V_2	4453
	compacted twice	V_3	4025
Valtra T190 + Opal 140; Valtra T190 + BS 400 A; U-650 + SUP-29	non-compacted	V_4	5800
	compacted once	V_5	4518
	compacted twice	V_6	4104
Valtra T190 + MCR-2,5	non-compacted	V_7	6016
	compacted once	V_8	4789
	compacted twice	V_9	4258
Valtra T190 + OA + AGPS-24DR	non-compacted	V_{10}	6268
	compacted once	V_{11}	5461
	compacted twice	V_{12}	4297
Valtra T190 + Opal 140 Valtra T190 + AGPS-24DR	non-compacted	V_{13}	5834
	compacted once	V_{14}	4557
	compacted twice	V_{15}	4182

Table 12. Seed yield for the autumn wheat crop

7. Conclusions and recomendations

Soil has an essential part in maintaining life on earth because it represents the support for the agriculture practice, creating the necessary conditions for obtaining the food products, due to its physical and biological properties, to its fertility, to its capacity to provide plants with the water and nutrients needed for their growth.

The intensification of the agricultural processes - mechanization, fertilization - led to a continuous degradation of soil, affecting five to seven million hectares each year. Sustainable agriculture could be a solution to this problem.

Sustainable agriculture is based on the soil conservation tillage system (SCTS). Within the unconventional soil tillage system moldboard plowing is deferred (completely or partially), the tillage works are limited and at least 15...30% of the vegetable debris is kept on the soil surface. The unconventional soil tillage system consists of very different methods: seeding in the untilled soil, reduced soil tillage, minimum soil tillage (when up to 30% of the vegetable debris is left on the soil surface), minimum tillage with vegetable mulch (more than 30% of the vegetable debris is left on the soil surface), ridge seeding, partial or strip tillage, deep loosening without furrow overturning etc.

The intensity of the anthropic soil compaction is affected by the type of agricultural machinery; compaction is promoted by the use of heavy machinery, with high wheel-soil contact pressures, by the increased number of passings, by the increased tire air pressure, by the agricultural traffic performed over wet soil. As far as the active parts for seedbed preparation are concerned, their destructive action over the structure elements of soil is of an utmost importance. The structure elements are destroyed through deformation, breaking, fragmentation, and cutting; in order to preserve soil structure one should comply with the technical recommendations of the equipment's manufacturer regarding the working speed and peripheral speed of the active parts.

In order to reproduce, in laboratory conditions, the working process of the active parts of the tillage equipment, a test rig was designed and built. The rig was used in order to study the soil - moldboard plough body interaction and the tire wheel-soil interaction; the results were then used to simulate the respective processes. The mathematical and physical simulations were performed by the means of CFD method. It was concluded that, in the case of the winged share type of active part, the maximum pressure would be recorded on the cutting edges. Based on the results of the simulations and on further field tests, new types of active parts will be developed; within the frame of conservative agriculture, this method allows the reduction of the time needed to produce new types of active parts.

The results of the mathematical and physical simulation were focused on soil, aiming to evaluate the compaction depth, the wheel indentation depth and the normal soil stress. The dynamic 3D simulation of a wheel rolling over an isotropic and non-linear soil produced truthful results regarding soil deformation and stresses at different depths, emphasizing the remanent soil stresses which lead to soil compaction and to the deterioration of its structure.

The laboratory results were validated by the field experiments, in which the effects of different agricultural equipments and of soil compaction over the penetration resistance, soil structure and yield were investigated.

Based on the results regarding the penetration resistance and bulk density, the variants (as presented in Table 7) were ranked as follows: V_{13} (1st place), V_4 (2nd place) and $V_{1\text{-witness}}$ (3rd place).

The analysis of the weighted average diameter and water stability of the aggregates led to the following rating: V_7 (1st place), V_{10} (2nd place) and V_{13} (3rd place).

The analysis of the seed yield led to the following rating: V_{10} (1st place), V_7 (2nd place) and V_{13} (3rd place).

When the indices referring to soil structure were considered, the best results were obtained by the variant V_7 (non compacted soil; tillage and sowing performed with the T190 + MCR-2.5 equipment); the second place was taken by variant V_{10} (non-compacted soil; tillage and sowing performed with the T190 + OA + AGPS-24DR equipment); variant V_{13} (plowing performed with the T190 + Opal 140 equipment, sowing performed with the T190 + AGPS-24DR equipment) was ranked the third.

Taking into account all the facts we consider that all decision makers, who are connected in anyway with soil (farmers, equipment producers, chemical products manufacturers, researchers), should be focused on the degradation of the arable layer and encourage agricultural technologies aiming to its preservation.

Author details

Ioan Tenu, Petru Carlescu, Petru Cojocariu and Radu Rosca
University of Agricultural Sciences and Veterinary Medicine, Iasi, Romania

8. References

[1] Abo-Elnor M., Hamilton, R., Boyle, J. T. (2004) Simulation of soil-blade interactions for sandy soil using advanced 3D finite element analysis. Soil&Tillage Research, 75: 61-73.

[2] Agoegwu S.N. (1994) Egusi-melon response to compaction due to traffic on a sandy loam soil. Proceedings of the 13th International Conference ISTRO, Denmark (1): 1-6.

[3] Block W.A. (1991) Analysis of soil stress under rigid wheel loading. Unpublished PhD Dissertation, Auburn University, Auburn AL.

[4] Canarache A. (1990) Physics of agricultural soils (in romanian). CERES Publishing House, Bucharest, Romania.

[5] Chi L., Kushwaha R.L. (1989) Finite element analysis of forces on a plane soil blade. Canadian Agricultural Engineering 31 (2): 135-140

[6] Eriksson J., Danfors B., Hakansson I. (1974) The effect of soil compaction on soil structure and crop yields. Bulletin 354, Swed. Inst. Agr. Eng., Uppsala, Sweden.

[7] Fervers C.W (2004) Improved FEM simulation model for a tire-soil interaction. Journal of Terramechanics 41(2-3): 87-100.

[8] Florea N. (2003) Degradation, protection and reclamation of soils and fields (in romanian). Universal Publishing House, Bucharest, Romania.

[9] Guş P., Rusu T. (2005) Sustainable development of agriculture (in romanian). Risoprint Publishing House, Cluj-Napoca, Romania.

[10] Hadas A., Larson W.E., Allmaras R.R. (1988) Advances in modeling machine-soil-plant interaction. Soil&Tillage Research, 11 (4): 349-372.
[11] Liu Y., Hou Z.M. (1985) Three-dimensional non-linear finite element analysis of soil cutting by narrow blades. Proceedings of the international conference on soil dynamics, Auburn, AL (2): 338-347.
[12] Shen J., Kushawa R.L. (1998) Soil-machine interaction: a finite perspective. Dekker, New York.
[13] Shmulevitch I., Asaf, Z., Rubinstein, D. (2007) Interaction between soil and a wide cutting blade using the discrete element method. Soil&Tillage Research, 97 (1): 37-50.
[14] Soane B.D., Bonne F.R (1986) The effect of tillage and traffic on soil structure. Soil&Tillage Research, 8: 303-306.
[15] Stout B.A. (editor) (1999). CIGH Handbook of agricultural engineering; vol. III – Plant production engineering. ASAE, St. Joseph, MI.
[16] Tanaka H., Momozu M., Oida A., Yamazaki M. (2000) Simulation of soil deformation and resistance at bar penetration by the distinct element method. Journal of Terramechanics, 37 (1): 41-56.
[17] Tolba M.L. (1987). Sustainable development-constraints and opportunities., Butterworth, London.
[18] Ţenu I., Cojocariu P., Cârlescu P., Roşca R., Leon D. (2010) Soil interaction with the active parts of the agricultural equipments (in Romanian). "Ion Ionescu de la Brad" Publishing House, Iaşi, Romania.
[19] Van Doren D., Unger P.W. (editors) (1982) Predicting tillage effects on soil physical properties and processes. ASA Special Publication 44, American Society of Agronomy and Soil Science Society of America Inc., Madison, WI, 198 pp.
[20] Wood R.K., Reeder, R.C., Morgan, M.T., Holmes, R.G. (1993) Soil physical properties as affected by grain cart traffic. Trans. of ASAE, 36 (1): 11-15.
[21] Yong R.N, Hanna A.W. (1977) Finite element analysis of plane soil cutting. Journal of Terramechanics, 14 (3):103-125.
[22] Zhang G.S., Chan K.Y., Oates A., Heenan D.P., Huang G.B. (2007) Relationship between soil structure and runoff/soil loss after 24 years of conservation tillage. Soil&Tillage Research, 92 (1-2):122-128.